

Generalised many body topological invariant and the unitary preparation of Chern insulators: An emergent bulk-boundary correspondence

Souvik Bandyopadhyay* and Amit Dutta

Department of Physics, Indian Institute of Technology Kanpur, Kanpur 208016, India

Building on the non-uniqueness of the macroscopic electric polarisation in the topological phase of a Chern insulator, we construct a many body Chern invariant. Under a smooth unitary temporal evolution, this quantity evolves with time and successfully reflects the topology of the out-of-equilibrium state of the system by assuming an integer-quantised value in the *adiabatic* limit. Considering a linear ramping of the staggered Semenoff mass of the paradigmatic Haldane model of graphene, we illustrate that starting from a trivial state, it is indeed possible to obtain a topologically non-trivial state even by an adiabatic unitary driving protocol. We further propose a counter-diabatic protocol that enables us to suppress the otherwise inevitable diabatic excitations generated while crossing the gapless quantum critical point. Notably, the corresponding emergence of an edge current in the final evolved state of the model under a semi-periodic boundary condition necessitates the application of a novel counter-diabatic field manifested as anisotropic hopping in the real space Hamiltonian. The generalised topology of this dynamical Chern invariant takes into account the dynamical occupation of instantaneous single-particle bands, and consequently ensconces an emergent bulk-boundary correspondence that is expected to manifest in experiments.

There has been a recent upsurge in theoretical [1–18] and experimental [19–28] studies probing the generation and manipulation of topological phases of many body quantum systems. Such topological phases are characterized and distinguished by different quantized values of a topological invariant which serves as a non-local order parameter. Distinct topological phases in thermodynamically large systems are necessarily separated by a quantum critical point (QCP) [29, 30]. Furthermore, the extremely robust protection of topological phases against external local perturbations opens up exciting possibilities for applications in topological quantum computation [31, 32] and controlling decoherence in out-of-equilibrium situations [33, 34].

The physical manifestation of ‘topology’ in symmetry protected topological insulators (SPTs) (see [11–13], for review) and Chern insulators (CIs) [14] is rendered in the form of topologically protected *boundary-localised* zero energy states when the bulk system is topologically non-trivial. This is the so-called bulk-boundary correspondence. Although the equilibrium topology of non-interacting quantum many body systems is well understood, comprehending the dynamical fate of equilibrium topology as well as characterising the topology of quantum systems which are driven out of equilibrium [35–47] and also the topology [48–51] associated with dynamical phase transitions [52–54] remain a challenging task in ongoing research.

Successfully designing a non-equilibrium topological system is a two-pronged process: a) dynamical generation of a topological Hamiltonian [35, 37]; b) preparation of the system in a topologically non-trivial dynamical state, e.g., in the ground state of the effective topological Hamiltonian, which is relatively difficult. Despite several works [55–65], the question of whether a out-of-equilibrium quantum many body system can be charac-

terised by an integer-quantised topological index, which also exhibits a bulk-boundary correspondence, is far from being settled.

Interestingly, for two-dimensional (2D) CI systems, a *no-go* theorem has been postulated [57], which states that the initial bulk topology of the model must not change under a smooth unitary transformation. This is an artefact of the temporal invariance of the dynamical Chern number (CN), constructed using the time evolved state of the system, under unitary driving. Nevertheless, following an adiabatic quench, the edge current eventually thermalizes to a value corresponding to the topology of the post-quench Hamiltonian [57–60]; thereby, implying the absence of an out-of-equilibrium bulk-boundary correspondence with respect to a topological index of the translationally invariant system. This fails to settle on any exclusive bulk topological nature of the emerging post-quench current in CIs, although it has been established for one-dimensional (1D) topological systems [63].

The question we address in this work is, whether it is possible to identify a generalised CN which can characterise the out-of-equilibrium state of a CI, under a smooth unitary evolution. We answer this in the affirmative by constructing a generalised invariant, extending the equilibrium property of the non-uniqueness of the Macroscopic electric polarisation (MEP) in the topological phase of a CI [66] to the non-equilibrium situation. We further show that this generalised CN is allowed to vary dynamically. Depending on time-dependent occupation of the eigenstates of the instantaneous Hamiltonian, it may dynamically assume an *integer-quantised* value when the system is ramped from the non-topological to the topological phase. Considering an *adiabatic* ramping of the Semenoff mass of the Haldane model [14], we establish the above claim where we also propound a counter-diabatic (CD) protocol

to suppress the non-adiabatic excitations. Furthermore, we explicitly demonstrate the topological nature of the emergent edge current and thus establish a bulk-boundary correspondence. To the best of our knowledge, the route, we unravel, to the unitary preparation of topological CI was not reported before.

MEP and Chern topology: The generalised CN is conjectured using the non-uniqueness of a component of MEP vector along a lattice direction due to the inability to define localized Wannier functions in the topological phase [66]. To elaborate, we evaluate the components of the MEP vector $\vec{P} = \sum_i P_i \hat{\mathbf{a}}_i$, where $\hat{\mathbf{a}}_i$ denotes the directions of the basis vectors of a 2D lattice (see [67] for a demonstration), i.e., for basis vectors $\hat{\mathbf{a}}_1$ and $\hat{\mathbf{a}}_2$, the MEP can be decomposed as,

$$\vec{P} = P_1 \hat{\mathbf{a}}_1 + P_2 \hat{\mathbf{a}}_2, \quad (1)$$

In the thermodynamic limit (see [66]),

$$P_i[\vec{k}_0] = \sum_{\alpha} \text{Im} \int_{BZ} \langle \psi_{k,\alpha} | \partial_{k_i} | \psi_{k,\alpha} \rangle dk_1 dk_2, \quad (2)$$

where \vec{k}_0 having components k_{01} and k_{02} along the reciprocal lattice directions, is chosen to be the origin of the Brillouin zone (BZ) and $|\psi_{k,\alpha}\rangle$'s are the respective occupied single particle bands labelled by “ α ” in the reciprocal space. The MEP of the system defined as an average of an $U(1)$ connection over the BZ, is directly related to the integrated charge current flowing in the system and Hall response under adiabatic evolution in trivial phases.

However, in the topological phase, for every adiabatic shift in the origin of the BZ [68], the MEP vector changes proportionally to the CN. If the system is in a pure state, for an infinitesimal shift in $\Delta \vec{k}_0$ in the origin \vec{k}_0 of the Brillouin zone,

$$\Delta P_i[\vec{k}_0] = P_i[\vec{k}_0 + \Delta \vec{k}_0] - P_i[\vec{k}_0] = 2\pi \epsilon_{ij} (\Delta k_0)_j \mathcal{C}, \quad (3)$$

where \mathcal{C} is the CN and ϵ_{ij} is the antisymmetric tensor. We utilize this non-uniqueness of the MEP to define the CN as,

$$\mathcal{C} = \epsilon_{ij} \frac{\Delta P_i[\vec{k}_0]}{2\pi \Delta k_{0j}}. \quad (4)$$

Generalised CN under unitary dynamics: We start from an initial eigenstate $|\psi(0)\rangle$ of a CI in the non-topological phase having $\mathcal{C} = 0$, which is subjected to an arbitrary unitary time dependent drive. To define the out-of-equilibrium CN, we extend the quantity defined in

Eq. (2), to a weighted average over the instantaneous bands of single-particle states (see [67]),

$$\tilde{P}_i = \sum_{\alpha} \text{Im} \int_{BZ} dk_1 dk_2 n_{\alpha}^k(t) A_i^k(|\phi_{k\alpha}(t)\rangle). \quad (5)$$

Here, $A_i^k(|\phi_{k\alpha}\rangle) = \langle \phi_{k\alpha} | \partial_{k_i} | \phi_{k\alpha} \rangle$ is the $U(1)$ gauge connection on the single-particle state $|\phi_{k\alpha}\rangle$ and the weights $n_{\alpha}^k(t)$ are the time dependent population of the instantaneous band ‘ α ’ as a function of momenta k .

We now proceed to define the dynamical CN as the change in the quantity \tilde{P}_i corresponding to a shift $\Delta \vec{k}_0$ in the BZ origin. This leads to the time-dependent CN,

$$\mathcal{C}^U(t) \propto \Delta \tilde{P}_1[\vec{k}_0] = -\Delta k_{02} \int_{k_{02}}^{k_{02}+1} dk_2 \partial_{k_2} \beta(k_2, t), \quad (6)$$

$$\text{where, } \beta(k_2, t) = -\sum_{\alpha} \text{Im} \int_{k_{01}}^{k_{01}+1} dk_1 n_{\alpha}^k(t) A_1^k(|\phi_{k\alpha}(t)\rangle). \quad (7)$$

At *equilibrium*, when any one of the bands is completely filled, the quantity \tilde{P}_i , reduces to the total MEP of the occupied band. In this situation, the CN defined in Eq. (4) and (6) is defined as a gauge invariant quantity which simply detects a branch change of the function $\beta(k_2)$ in the closed interval $k_2 \in [0, 1] \equiv \mathcal{S}^1$; which equivalently counts the winding of a uni-directional $U(1)$ Berry phase $\beta(k_2)$ along the \mathcal{S}^1 direction k_2 [66, 67]. By fixing a gauge, such that the quantity $\beta(k_2)$ remains continuous for all $k_2 \in [0, 1]$ in a topological phase, the function $\beta(k_2)$ exhibits a branch change proportional to the CN, at the endpoints of the BZ, i.e. $\mathcal{C} \propto \beta(k_2 + 1) - \beta(k_2)$. Even under an arbitrary gauge choice, the existence of a branch singularity in the map $k_2 \in [0, 1] \rightarrow \beta(k_2)$, signals the Chern non-triviality of the system. To elaborate, the sudden jump Δ in the $\beta(k_2)$ function in a non-trivial phase must be integer multiples of 2π where the integer multiple being the CN itself, precisely characterizes the homotopy class of the map, i.e.,

$$\Delta = -2\pi \mathcal{C}, \quad \mathcal{C} \in \mathcal{I}. \quad (8)$$

However, for a general *out-of-equilibrium* situation, the quantity $\mathcal{C}^U(t)$ defined in Eq. (6) fails to capture the $U(1)$ gauge connection of the time-evolved quantum state, as a single instantaneous band may not be completely occupied far from equilibrium [69]. Nonetheless, for an *adiabatic* protocol dynamically exchanging the Chern character of the two bands, the $U(1)$ connection is over the many body projected band i.e., the instantaneous band which is nearly completely filled. This allows for the CN to vary in time. Thus, in the perfectly adiabatic situation, the MEP assumes the exact $U(1)$ form,

$$\tilde{P}_i = \text{Im} \int_{BZ} dk_1 dk_2 A_i^k(|\phi_{ks}(t)\rangle), \quad (9)$$

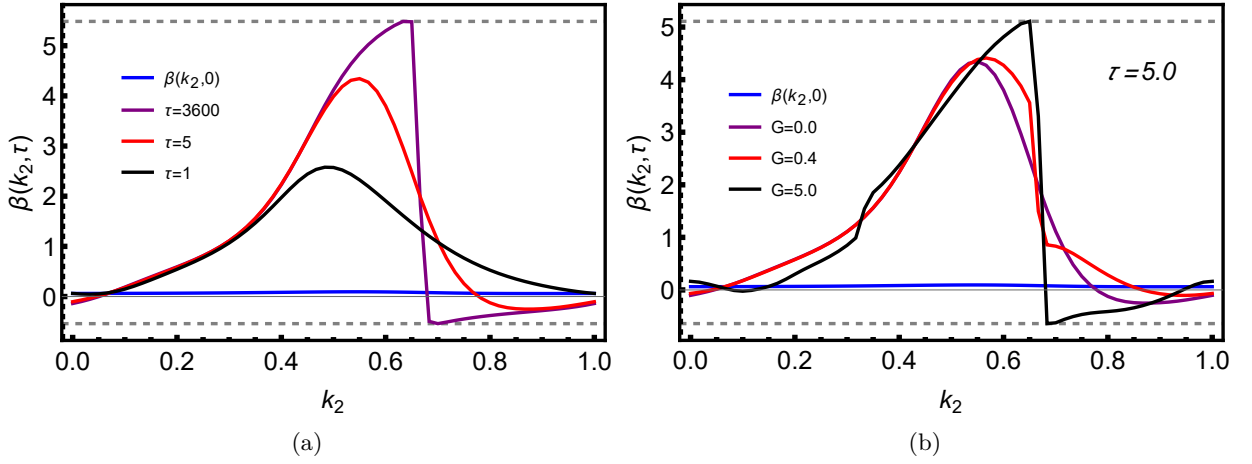


Figure 1: (a) Emergence of a sharp branch singularity in the function $\beta(k_2, \tau)$. The sharp jump in the $\beta(k_2, \tau)$ function for an adiabatic driving protocol (Eq. (10)) starting from an initial trivial state, demonstrates the topological non-triviality of the final time evolved state. The magnitude of the jump shown by the distance between the horizontal dashed lines is $\Delta = -0.96 \times 2\pi$. The initial and the final Hamiltonian is chosen such that, nearest neighbour hopping $t_1 = 1.0$, next-nearest neighbour hopping $t_2 = 0.5$, flux through each plaquette $\phi = \pi/4$, $M_i = 3\sqrt{3}t_2 + 2.5$, $M_f = 3\sqrt{3}t_2 - 2.5$. (b) The $\beta(k_2, \tau)$ function exhibits a sharp branch singularity in the post-quench state for a drive employing shortcut to adiabaticity (Eqs. (11)-(12)) with increasing control field strength G . The magnitude of the jump shown by the distance between the horizontal dashed lines is $\Delta = -0.92 \times 2\pi$ with the set of quench parameters as in (a). The quenching period is chosen to be $\tau = 5.0$ which is much shorter than the adiabatic time scale ($\tau \simeq 3600$). Periodic boundary conditions are imposed with a grid size of 60×60 lattice sites in both the figures.

over the filled band $\alpha = s$.

The motivation behind incorporating the non-equilibrium occupations in Eq. (5) is the following: the topological classification of out of equilibrium states is directly connected to the evolution of particle currents generated in the time dependent state of the system. For the topological invariant to conform with the adiabatic edge current dynamics, it is essential to take note of the time evolution of the current operator which depends on the instantaneous Hamiltonian [57, 67, 70].

Illustration with Haldane model: To exemplify, we linearly quench the Semenoff mass $M(t)$ of a Haldane model ([67]),

$$H^k(t) = h_x \sigma_x + h_y \sigma_y + h_z(t) \sigma_z, \quad \text{with} \quad (10)$$

$$M(t) = M_i - (M_i - M_f) \frac{t}{\tau},$$

in time $t \in [0, \tau]$. Initially ($t = 0$), the system is in a pure state $|\psi_k(0)\rangle$ which is the ground state of the initial (non-topological) Hamiltonian $H^k(0)$ with $M(0) = M_i$ and the final value $M(\tau) = M_f$ corresponds to a topological Hamiltonian; thus, the system is ramped across a QCP during the evolution.

We evaluate the function $\beta(k_2, \tau)$ in the final state $|\psi_k(t)\rangle$ at $t = \tau$ generated following the evolution under the protocol in Eq. (10). As shown in Fig. 1a the function

$\beta(k_2, \tau)$ evaluated on the circle $k_2 \in [0, 1]$ develops a sharp branch singularity of nearly quantized integral multiple of 2π , only when the quench approaches the adiabatic limit. As discussed above, the existence of this sharp branch shift in $\beta(k_2, \tau)$, signals the topological non-triviality of the final state of the system.

Counter-diabatic protocol: During the passage through a gapless QCP, the adiabaticity criteria necessarily breaks down in the thermodynamic limit and diabatic excitations are inevitable. Nevertheless, the application of a control perturbation [70–72] may open up a gap even at the QCPs guaranteeing adiabaticity throughout the evolution, thereby, allowing for a much more efficient preparation of a topological state. The protocol we propose is the following:

$$H^k(t) = h_x \sigma_x + h_y \sigma_y + h_z(t) \sigma_z + B_x(t) \sigma_x, \quad (11)$$

$$M(t) = M_i - (M_i - M_f) \frac{t}{\tau},$$

where the control (counter-diabatic) field is chosen as:

$$B_x(t) = G \sin\left(\frac{\pi t}{\tau}\right), t \in [0, \tau]; B_x(0) = B_x(\tau) = 0. \quad (12)$$

Again the initial system is in a trivial state while the final is expected to be topological one. Starting from the ground state of the initial Hamiltonian, we probe the emergence of topology in the out of equilibrium

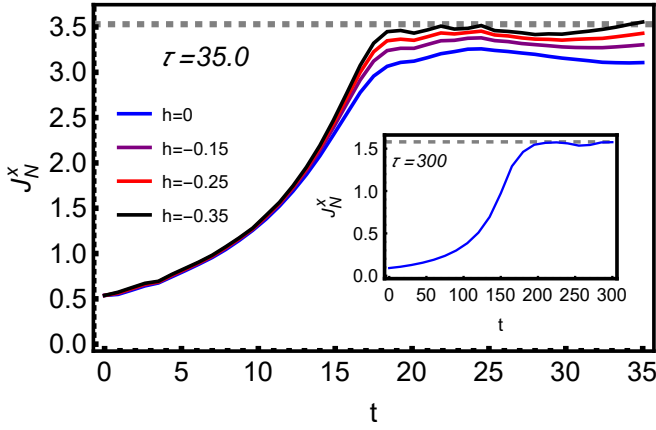


Figure 2: The time evolution of the current J_N^x through an arm-chair edge of the Haldane model with semi-open boundary conditions (periodic about the x-direction and open in y-direction [67]) under a linear quench with the counter diabatic mass generation as in Eq. (11) with $t_1 = 2.0$, $t_2 = 1.0$, $\phi = \pi/4$, $M_i = 3\sqrt{3}t_2 + 2.5$, $M_f = 0$, for a 18×18 lattice. “ h ” is the strength of the anisotropic hopping (see [67]) introduced in the real space lattice which in turn generates a CD mass. (Inset) The adiabatic evolution of the edge-current vide the protocol in Eq. (10) with initial and final parameters same as in Fig. 1a for a 16×16 lattice. At $t = \tau$, the edge-current (solid curve) thermalizes to its equilibrium topological value (dashed line) in both protocols.

state. In Fig. 1b, we observe that again the post-quench state develops a sharp branch singularity showing near quantisation of the jump Δ (i.e., $C^U(\tau) \simeq 1$) however in a much shorter duration of quench than that in the case of a perfectly adiabatic protocol.

Bulk-boundary correspondence: The topological nature of the post quench state is manifested in the emergence of localized edge currents J_N^x under semi-periodic boundary conditions in a system having $N \times N$ atoms, as demonstrated in Fig. 2. The CD mass in Eq. (11) can be generated experimentally through an anisotropic strain [73, 74] in the real space lattice which in turn induces an anisotropy in the nearest neighbour hopping strength [67]. The edge therefore bears the signature of the bulk topology both under adiabatic and CD dynamics [75].

In conclusion, we have achieved the dynamical preparation of topological states of a CI within a unitary set up. The dynamical CN evolves with time unlike that defined in Ref. [57] and assumes an integer-quantised value, though not for an arbitrary protocol, nevertheless for a perfectly adiabatic evolution. Starting with the ground state of the trivial Haldane Hamiltonian, we illustrate the emergence of a sharp branch singularity in the weighted average of the unidirectional Berry phase confirming

that the evolved final state is indeed topological. This is further corroborated by an emergent bulk-boundary correspondence. The CD field, we propose, can be experimentally generated in graphene and borophene lattices by applying anisotropic strains in particular bond directions or through dynamical gap manipulations as explored theoretically and experimentally in [76–80].

We specially acknowledge Utso Bhattacharya, Arijit Kundu, Somnath Maity, Sougato Mardanya, Anatoli Polkovnikov and Diptiman Sen for helpful discussions and critical comments. We thank Sourav Bhattacharjee for critical reading of the manuscript. SB acknowledges PMRF, MHRD India for financial assistance. AD acknowledges financial support from SPARC program, MHRD, India. We also acknowledge ICTS, Bangalore, India where some part of the work was done.

* souvik@iitk.ac.in

- [1] A. Kitaev, Phys.-Usp. **44**, 131 (2001).
- [2] C. L. Kane and E. J. Mele, Phys. Rev. Lett. **95**, 226801(2005).
- [3] B. A. Bernevig, T. L. Hughes, S-C. Zhang, Science, **314**, 5806 (2006).
- [4] L. Fu and C. L. Kane, Phys. Rev. Lett. **100**, 096407 (2008).
- [5] C. W. Zhang, S. Tewari, R. M. Lutchyn, and S. Das Sarma, Phys. Rev. Lett. **101**, 160401 (2008).
- [6] M. Sato, Y. Takahashi, and S. Fujimoto, Phys. Rev. Lett. **103**, 020401 (2009).
- [7] J. D. Sau, R. M. Lutchyn, S. Tewari, and S. Das Sarma, Phys. Rev. Lett. **104**, 040502 (2010).
- [8] J. D. Sau, S. Tewari, R. M. Lutchyn, T. D. Stanescu, and S. Das Sarma, Phys. Rev. B **82**, 214509 (2010).
- [9] R. M. Lutchyn, J. D. Sau, and S. Das Sarma, Phys. Rev. Lett. **105**, 077001 (2010).
- [10] Y. Oreg, G. Refael, and F. von Oppen, Phys. Rev. Lett. **105**, 177002 (2010).
- [11] J. E. Moore, Nature **464**, 194 (2010).
- [12] S-Q. Shen, *Topological Insulator*, Springer (2012).
- [13] B. A. Bernevig with T. L. Hughes, *Topological Insulators and Topological Superconductors*, Princeton University Press, Princeton (2013).
- [14] F. D. M. Haldane, Phys. Rev. Lett. **51**, 605 (1983).
- [15] X.G. Wen, Adv. Phys. **44**, 405 (1995).
- [16] A. Kitaev, Annals of Physics, **303**, Issue 1, (2003).
- [17] A. Kitaev, Annals of Physics, **321**, Issue 1 (2006).
- [18] M. Levin and X.G. Wen, Phys. Rev. Lett. **96**, 110405 (2006).
- [19] V. Mourik, K. Zuo, S. M. Frolov, S. R. Plissard, E. P. A. M. Bakkers, and L. P. Kouwenhoven, Science **336**, 1003 (2012).
- [20] L. P. Rokhinson, X. Liu, and J. K. Furdyna, Nat. Phys. **8**, 795 (2012).
- [21] M. T. Deng, C. L. Yu, G. Y. Huang, M. Larsson, P. Caroff, and H. Q. Xu, Nano Lett. **12**, 6414 (2012).
- [22] A. Das, Y. Ronen, Y. Most, Y. Oreg, M. Heiblum, and H. Shtrikman, Nat. Phys. **8**, 887 (2012).
- [23] H. O. H. Churchill, V. Fatemi, K. Grove-Rasmussen, M.

- T. Deng, P. Caroff, H. Q. Xu, and C. M. Marcus, Phys. Rev. B **87**, 241401(R) (2013).
- [24] A. D. K. Finck, D. J. Van Harlingen, P. K. Mohseni, K. Jung, and X. Li, Phys. Rev. Lett. **110**, 126406 (2013).
- [25] J. Alicea, Rep. Prog. Phys. **75**, 076501 (2012).
- [26] M. Leijnse and K. Flensberg, Semicond. Sci. Technol. **27**, 124003 (2012).
- [27] C. W. J. Beenakker, Annu. Rev. Con. Mat. Phys. **4**, 113 (2013).
- [28] T. D. Stanescu and S. Tewari, J. Phys.: Condens. Matter **25**, 233201 (2013).
- [29] S. Sachdev, *Quantum Phase Transitions*, Cambridge University Press, Cambridge (2010).
- [30] A. Dutta, G. Aeppli, B. K. Chakrabarti, U. Divakaran, T. F. Rosenbaum, D. Sen, *Quantum Phase Transitions in Transverse Field Spin Models*, Cambridge University Press, Cambridge (2015).
- [31] A. Kitaev and C. Laumann, arXiv:0904.2771, (2016).
- [32] V. Lahtinen, J. K. Pachos, SciPost Phys. **3**, 021 (2017).
- [33] B. Damski, H. T. Quan, W. H. Zurek Phys. Rev. A **83**, 062104, (2011).
- [34] T Nag, U Divakaran, A Dutta, Phys. Rev. B **86**, 020401. (2012).
- [35] T. Oka and H. Aoki, Phys. Rev. B **79**, 081406 (R) (2009).
- [36] A. Bermudez, D. Patane, L. Amico, and M. A. Martin Delgado, Phys. Rev. Lett. **102**, 135702 (2009).
- [37] T. Kitagawa, T. Oka, A. Brataas, L. Fu, and E. Demler, Phys. Rev. B **84**, 235108 (2011).
- [38] N. H. Lindner, G. Refael, and V. Galitski, Nat. Phys. **7**, 490 (2011).
- [39] A. A. Patel, S. Sharma, and A. Dutta, Eur. Phys. J. B **86**, 367 (2013).
- [40] A Rajak, A Dutta, Phys. Rev. E **89**, 042125 (2014).
- [41] M. Thakurathi, A. A. Patel, D. Sen, and A. Dutta, Phys. Rev. B **88**, 155133 (2013).
- [42] A. Kundu and B. Seradjeh, Phys. Rev. Lett. **111**, 136402 (2013).
- [43] J. Cayssol, B. Dora, F. Simon, and R. Moessner, Phys. Status Solidi RRL **7**, 101 (2013).
- [44] M.S. Rudner, N.H. Lindner, E. Berg, and M. Levin, Phys. Rev. X **3**, 031005 (2013).
- [45] L. E. F. Foa Torres, P. M. Perez-Piskunow, C. A. Balseiro, and G. Usaj, Phys. Rev. Lett. **113**, 266801 (2014).
- [46] H. Dehghani, T. Oka, and A. Mitra, Phys. Rev. B **91**, 155422 (2015).
- [47] J.H. Wilson, J. C.W. Song, and G. Refael, Phys. Rev. Lett. **117**, 235302 (2016).
- [48] Szabolcs Vajna, Balazs Dora, Phys. Rev. B **91**, 155127 (2015).
- [49] U Bhattacharya, A Dutta, Physical Review B **95**, 184307 (2017).
- [50] J.C. Budich and M. Heyl, Phy. Rev. B **93**, 085416 (2016).
- [51] U Bhattacharya, A Dutta, Phys. Rev. B **96**, 014302 (2017).
- [52] M. Heyl, A. Polkovnikov, and S. Kehrein Phys. Rev. Lett. **110**, 135704 (2013).
- [53] S Sharma, U Divakaran, A Polkovnikov, A Dutta, Phys. Rev. B **93**, 144306 (2016).
- [54] M Heyl, Reports on Progress in Physics **81**, 054001 (2018).
- [55] M. S. Foster, M. Dzero, V. Gurarie, and E. A. Yuzbashyan, Phys. Rev. B **88**, 104511 (2013).
- [56] M. S. Foster, V. Gurarie, M. Dzero, and E. A. Yuzbashyan, Phys. Rev. Lett. **113**, 076403 (2014).
- [57] L. D'Alessio and M. Rigol, Nature Communications **6**, 8336 (2015).
- [58] M.D. Caio, N.R. Cooper, and M.J. Bhaseen, Phys. Rev. Lett. **115**, 236403 (2015).
- [59] U. Bhattacharya, J. Hutchinson, and A. Dutta, Phys. Rev. B **95**, 144304 (2017).
- [60] S. Mardanya, U. Bhattacharya, A. Agarwal, and A. Dutta, Phys. Rev. B **97**, 115443 (2018).
- [61] M. McGinley and N.R. Cooper, Phys. Rev. Lett. **121**, 090401 (2018).
- [62] S. Bandyopadhyay, U. Bhattacharya and A. Dutta, Phys. Rev. B **100**, 054305 (2019).
- [63] S. Bandyopadhyay and A. Dutta, Phys. Rev. B **100**, 144302 (2019).
- [64] R. Verresen, arXiv: 2003.05453 (2020)
- [65] L. Pastori, S. Barbarino, and J. C. Budich, arXiv:2003.07874 (2020).
- [66] S. Coh and D. Vanderbilt, Phys. Rev. Lett. **102**, 107603 (2009).
- [67] See Supplemental Material at [URL to be inserted by publisher]
- [68] An adiabatic shift implies that the occupation of each band remain invariant.
- [69] This is reflected in β defined Eq. (7), as a weighted average of $U(1)$ Berry phases over all instantaneous bands.
- [70] M. Bukov and A. Polkovnikov, Phys. Rev. A **90**, 043613 (2014).
- [71] D. Sels and A. Polkovnikov, Proc. Natl. Acad. Sci. U.S.A. **114**, E3909 (2017).
- [72] P.W. Claeys, M. Pandey, D. Sels, and A. Polkovnikov, Phys. Rev. Lett. **123**, 090602 (2019).
- [73] V.M. Pereira, A.H. Castro Neto, Phys. Rev. Lett. **103**, 046801 (2009).
- [74] M. R. Masir, D. Moldovan, and F. M. Peeters, Solid State Commun. **175-176**, 76 (2013).
- [75] The transition reflected in the edge-behavior is expected to be sharper with increasing system size.
- [76] M.O. Leyva and G.G. Naumis, Phys. Rev. B **93**, 035439 (2016).
- [77] M.O. Leyva and G.G. Naumis, Phys. Rev. B **88**, 085430 (2013).
- [78] H.T. Yang, J. Phys.: Condens. Matter **23** 505502 (2011).
- [79] N. Levy *et.al.*, Science **329**, 5991 (2010).
- [80] V.G.I. Sierra, J.C.S. Santana, A. Kunold, and G.G. Naumis, Phys. Rev. B **100**, 125302 (2019).

Supplemental Material on “Generalised many body topological invariant and the unitary preparation of Chern insulators: An emergent bulk-boundary correspondence”

A BRIEF REVIEW ON HALDANE MODEL OF GRAPHENE :

The bare Hamiltonian for the Haldane model [S1] is obtained by breaking the time reversal and sublattice of graphene ,

$$H_{\alpha,\beta,n,m}^0 = -t_1 \sum_{\langle m\alpha,n\beta \rangle} a_{m,\alpha}^\dagger a_{n,\beta} + M \sum_n a_{n,A}^\dagger a_{n,A} - M \sum_n a_{n,B}^\dagger a_{n,B} - \sum_{\langle\langle m\alpha,n\alpha \rangle\rangle} t_2 e^{i\phi} a_{m,\alpha}^\dagger a_{n,\alpha} + h.c., \quad (S1)$$

where the real nearest neighbour (N1) hopping t_1 (with $t_2 = 0, M = 0$) comprises the bare graphene Hamiltonian; the indices n and α represent site and sublattice respectively. The diagonal staggered mass (Semenoff mass) M explicitly breaks the sublattice symmetry of the model. Further the complex next nearest neighbour (N2) hopping term t_2 , is applied such that the time reversal symmetry is broken in the next nearest neighbour hopping while the net flux through each plaquette remains zero. The Haldane model is known to exhibit non-trivial Chern topology when its ground state is completely filled depending on the parameters M, t_1, t_2 and ϕ .

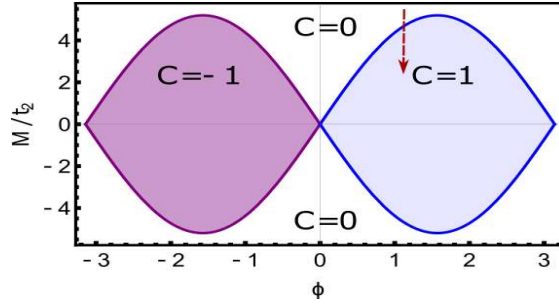


Figure S1: (Color online) The topological phase diagram of the Haldane model with $t_1 = 1.0$. The distinct topological phases are separated by quantum critical lines on which the parameter values are such that the system becomes gapless. The parameter regions showing non-zero values of the Chern number (C) are topologically non-trivial. The red arrow show the direction of the initial and final region of the quench employed in the manuscript.

Interestingly, the Haldane model with explicitly broken time reversal symmetry is known to host topologically non-trivial phases for certain parameter regions. The topology of the Hamiltonian is essentially the homotopy classification of the map $(k_1, k_2) \rightarrow H^k(k_1, k_2)$ in reciprocal space and is characterized by the gauge invariant Chern topological invariant,

$$C = \frac{1}{(2\pi)^2} \int_{BZ} dk_1 dk_2 \mathcal{F}_{12}(|\psi_k\rangle), \quad (S2)$$

where, $\mathcal{F}_{12}(|\psi_k\rangle)$ is the $U(1)$ curvature defined over the ground state $|\psi_k\rangle$ of the Hamiltonian H^k , i.e.,

$$\mathcal{F}_{12}(|\psi_k\rangle) = \partial_{k_2} \langle \psi_k | \partial_{k_1} | \psi_k \rangle - \partial_{k_1} \langle \psi_k | \partial_{k_2} | \psi_k \rangle. \quad (S3)$$

The Chern invariant is integer quantized as long as the Hamiltonian H^k does not approach a QCP where the Chern number becomes ill-defined. Different integer values of the Chern number characterize distinct topological phases separated by QCPs (see Fig. S1).

Each point on the Bravias lattice can be referenced in terms of the Bravias lattice vectors, i.e.,

$$\vec{a} = n_1 \vec{a}_1 + n_2 \vec{a}_2, \quad (S4)$$

where the vectors \vec{a}_1 and \vec{a}_2 span the Bravias lattice and n_1, n_2 are integers. We choose the vectors \vec{a}_1 and \vec{a}_2 to be the next nearest neighbour hopping vectors such that,

$$\begin{aligned} \vec{a}_1 &= \vec{\Delta}_{22}, \\ \vec{a}_2 &= -\vec{\Delta}_{21}, \end{aligned} \quad (S5)$$

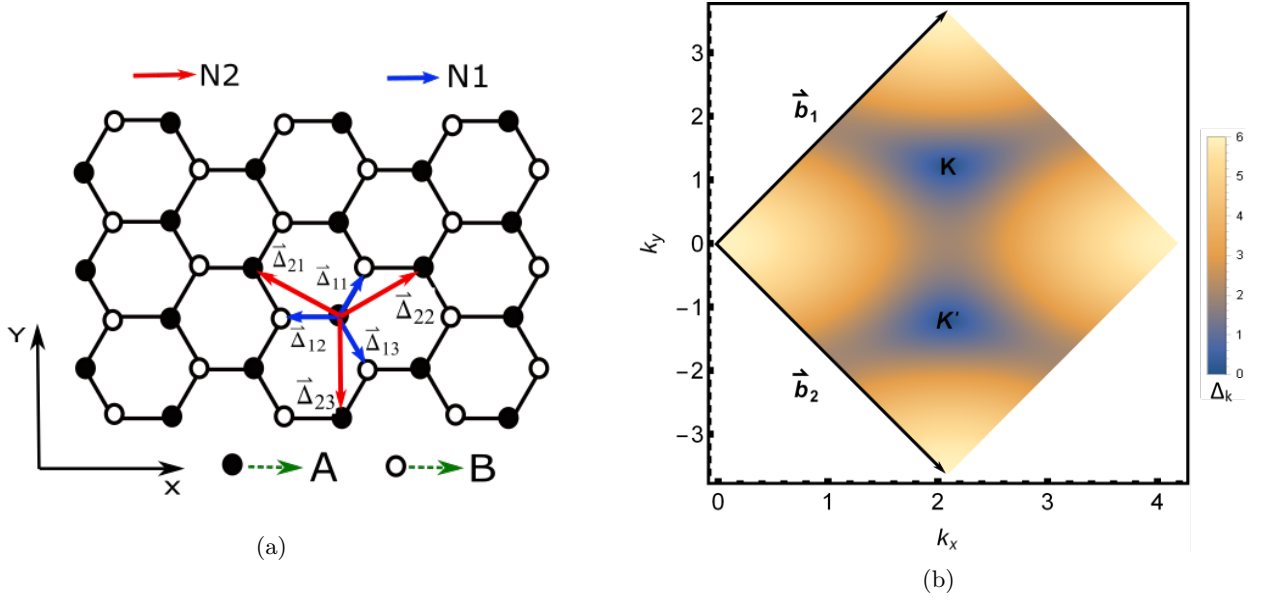


Figure S2: (Color online) (a) The hexagonal graphene lattice showing the nearest neighbour (N1) and next-nearest neighbour (N2) hopping vectors $\vec{\Delta}_{1i}$ and $\vec{\Delta}_{2i}$, respectively, where the lattice constant is set to be $a = 1$. The hollow and the filled atoms represent the B and A sublattices respectively. (b) The Brillouin zone of graphene spanned by the reciprocal lattice vectors \vec{b}_1 and \vec{b}_2 containing two inequivalent Dirac points K and K' (the cartesian directions has been labelled by k_x and k_y respectively). The color density shows the absolute value of the bandgap Δ_k of the reciprocal space graphene Hamiltonian showing vanishing gaps at the Dirac points for a 600×600 lattice size having the N1 hopping strength $t_1 = 1.0$ and the N2 hopping $t_2 = 0$.

where $\vec{\Delta}_{2i}$ are the N2 vectors as shown in Fig. S2a.

Invoking the discrete translational invariance of the Hamiltonian one can employ a discrete Fourier transform to decouple the Hamiltonian $H(t)$ in momentum space. The reciprocal space is spanned by the reciprocal lattice vectors \vec{b}_1 and \vec{b}_2 , i.e. every reciprocal lattice point can be represented as,

$$\vec{b} = k_1 \vec{b}_1 + k_2 \vec{b}_2, \quad (\text{S6})$$

where, $k_1, k_2 \in [0, 1)$. We choose a rhomboidal Brillouin zone spanned by reciprocal lattice vectors \vec{b}_1 and \vec{b}_2 (see Fig. S2b) containing two independent Dirac points K and K' . In our choice of representation,

$$\vec{b}_1 = \frac{2\pi}{3a} \{1, \sqrt{3}\} \quad \text{and} \quad \vec{b}_2 = \frac{2\pi}{3a} \{1, -\sqrt{3}\}, \quad (\text{S7})$$

where we have chosen $a = 1$. The corresponding inequivalent Dirac points in the Brillouin zone shown in Fig. S2b are given by,

$$K = \frac{2\pi}{3} \left(1, \frac{1}{\sqrt{3}}\right) \quad \text{and} \quad K' = \frac{2\pi}{3} \left(1, -\frac{1}{\sqrt{3}}\right). \quad (\text{S8})$$

The bare Haldane Hamiltonian gets decoupled in the momentum space where $H^0(k)$ can be written in the basis $|k, A\rangle$ and $|k, B\rangle$ as,

$$H^0(k) = \vec{h}(k) \cdot \vec{\sigma} = h_x(k) \sigma_x + h_y(k) \sigma_y + h_z(k) \sigma_z, \quad (\text{S9})$$

such that,

$$\begin{aligned} h_x(k) &= -t_1 \sum_{i=1}^3 \cos(\vec{k} \cdot \vec{\Delta}_{1i}), \\ h_y(k) &= -t_1 \sum_{i=1}^3 \sin(\vec{k} \cdot \vec{\Delta}_{1i}), \\ h_z(k) &= M - t_2 \sin \phi \sum_{i=1}^3 \sin(\vec{k} \cdot \vec{\Delta}_{2i}), \end{aligned} \quad (\text{S10})$$

$\vec{\Delta}_{1i}$ and $\vec{\Delta}_{2i}$ are the nearest neighbour and next nearest neighbour lattice vectors respectively (see Fig. S2a) chosen to be,

$$\begin{aligned} \vec{\Delta}_{11} &= \frac{a}{2}\{1, \sqrt{3}\}, \quad \vec{\Delta}_{12} = \{-a, 0\}, \quad \vec{\Delta}_{13} = \frac{a}{2}\{1, -\sqrt{3}\} \quad \text{and}, \\ \vec{\Delta}_{21} &= \frac{a}{2}\{-3, \sqrt{3}\}, \quad \vec{\Delta}_{22} = \frac{a}{2}\{3, \sqrt{3}\}, \quad \vec{\Delta}_{23} = \{0, -a\sqrt{3}\}, \end{aligned} \quad (\text{S11})$$

in the cartesian frame (Fig. S2a) where we have chosen the lattice parameter $a = 1$. Note that we have used Eq. (S9) in Eq. (15) of the main text where the Semenoff mass term which appears only in $h_z(k)$ is linearly ramped across the quantum critical point from the non-topological to the topological phase.

MACROSCOPIC POLARISATION, CHERN NUMBER AND ITS OUT-OF-EQUILIBRIUM GENERALISATION

We evaluate the macroscopic electric polarisation vector [S2] of the system in the directions of the lattice basis vectors (Eq. (S5) and Fig. S2a),

$$\vec{P} = \sum_i P_i \hat{\mathbf{a}}_i, \quad (\text{S12})$$

where $P_i = \langle \hat{X}_i \rangle$, and $\hat{\mathbf{a}}_i$ are the lattice basis vectors. The quantity $\hat{X}_i = \sum_n x_i^n \hat{a}_n^\dagger \hat{a}_n$ is the many-body position operator where x_i^n denotes the coordinate of an atom at the n^{th} site along the i^{th} lattice direction with \hat{a}_n^\dagger being the corresponding fermionic creation operator at that site. The expectation is taken over a fermionic many body state. The translation operator in the i^{th} direction under periodic boundary conditions,

$$\hat{T}_i(\delta_i) = e^{i\delta_i \hat{X}_i}, \quad (\text{S13})$$

where we choose $\delta_i = 2\pi/N_i$, N_i being the dimension of the system in the i^{th} direction. The periodicity of the exponential enforces periodic boundary conditions on the lattice. Therefore, under periodic boundary conditions and in the thermodynamic limit, the macroscopic polarisation of the system assumes the following form,

$$P_i = \text{Im} \ln \langle \hat{T}_i \rangle, \quad (\text{S14})$$

where the expectation is taken over the full many-body state of the system. In the thermodynamic limit, this compactified definition of the macroscopic polarisation reduces to the conventional bulk polarisation of the system. This is evident from the fact that, for a many-particle pure state, $|\Psi\rangle$ (which is a slater determinant of the occupied single-particle states),

$$P_i = \text{Im} \ln \langle \hat{T}_i \rangle = \text{Im} \ln \det U = \text{Im} \ln e^{\text{Tr} \ln U}, \quad (\text{S15})$$

where the matrix U contains all the overlap of the single-particle matrix T_i between the occupied single particle states, i.e.,

$$U_{mn} = \langle \psi_m | T_i | \psi_n \rangle \implies (U)_{k\alpha, k'\beta} = \langle \psi_{k_i+\delta_i, \alpha} | \psi_{k, \alpha} \rangle \simeq e^{-i(A_i^k)_{\alpha\alpha} \delta_i}, \quad (\text{S16})$$

where k denotes the single-particle momenta while α and β are the band indices and $(A_i^k)_{\alpha\alpha}$ is the $U(1)$ connection of the α^{th} occupied band. In the thermodynamic limit ($\delta_i \rightarrow 0$), retaining only terms of linear order in δ_i , one obtains,

$$P_i = \sum_{\alpha} \text{Im} \int_{BZ} \langle \psi_{k,\alpha} | \partial_{k_i} | \psi_{k,\alpha} \rangle dk_1 dk_2, \quad (\text{S17})$$

which is the macroscopic polarisation of the system.

The Chern invariant conventionally defined as,

$$C = \frac{1}{(2\pi)^2} \int_{BZ} dk_1 dk_2 [\partial_{k_1} \langle \psi_k | \partial_{k_2} | \psi_k \rangle - \partial_{k_2} \langle \psi_k | \partial_{k_1} | \psi_k \rangle], \quad (\text{S18})$$

can be recast to the form,

$$C = \frac{1}{(2\pi)^2} \int_{k_{20}}^{k_{20}+1} dk_2 \partial_{k_2} \int_{k_{10}}^{k_{10}+1} dk_1 \langle \psi_k | \partial_{k_1} | \psi_k \rangle = -\frac{1}{(2\pi)^2} \int_{k_{20}}^{k_{20}+1} dk_2 \partial_{k_2} \beta(k_2), \quad (\text{S19})$$

where,

$$\beta(k_2) = - \int_{k_{10}}^{k_{10}+1} dk_1 \langle \psi_k | \partial_{k_1} | \psi_k \rangle. \quad (\text{S20})$$

The Chern number therefore essentially counts the $U(1)$ winding of the map,

$$\mathcal{S}^1 : k_2 \in [0, 1] \rightarrow \mathcal{S}^1 : \beta(k_2). \quad (\text{S21})$$

Meanwhile, the change in macroscopic electric polarisation under an infinitesimal adiabatic shift in the Brillouin zone origin evaluates to the exact same quantity,

$$P_1[\vec{k}_0 + \Delta \vec{k}_0] - P_1[\vec{k}_0] = \Delta k_{02} \int_{k_{02}}^{k_{02}+1} dk_2 \partial_{k_2} \beta(k_2). \quad (\text{S22})$$

This shows that in a Chern insulator which is in the topologically non-trivial state ($C \neq 0$), the macroscopic polarisation vector cannot be uniquely defined. This is because a non-trivial Chern insulator is not an insulator in the strict sense due to the chiral conducting edge channels [S2].

In the main text, we consider an arbitrary unitary drive starting from an initial eigenstate state $|\psi(0)\rangle$ of the Chern insulator (this ensures half-filling of the initial single-particle states) in the non-topological phase with $\mathcal{C} = 0$ (as shown in Fig. S1) such that the time evolved state is,

$$|\psi(t)\rangle = U(t, 0) |\psi(0)\rangle, \quad (\text{S23})$$

where $U(t, 0)$ is the evolution operator generated by an instantaneous hermitian Hamiltonian $H(t)$. Translating to Fourier space, the instantaneous eigenmodes $|\phi_{k\alpha}(t)\rangle$ of the instantaneous Hamiltonian $H_k(t)$ satisfy,

$$H_k(t) |\phi_{k\alpha}(t)\rangle = E_{k\alpha}(t) |\phi_{k\alpha}(t)\rangle, \quad (\text{S24})$$

with eigenvalues $E_{k\alpha}(t)$, for all $k \in BZ$. and α denotes the band index.

As discussed in Eq. (S17), the electric polarisation in the i^{th} direction for an arbitrary pure quantum many-body state $|\chi\rangle$ reduces to the average of the quantity,

$$\Lambda_i^k = \sum_{\alpha} A_i^k(|\chi_{k\alpha}\rangle), \quad (\text{S25})$$

over the complete Brillouin zone and summed over all the occupied single particle states $|\chi_{k\alpha}\rangle$. Here, $A_i^k(|\chi_{k\alpha}\rangle)$ is the $U(1)$ gauge connection on the state $|\chi_{k\alpha}\rangle$ i.e.,

$$A_i^k(|\chi_{k\alpha}\rangle) = \langle \chi_{k\alpha} | \partial_{k_i} | \chi_{k\alpha} \rangle. \quad (\text{S26})$$

In the out-of-equilibrium situation, we extend the quantity defined in Eq. (S17) as a weighted average over the instantaneous single-particle bands,

$$\tilde{P}_i = \sum_{\alpha} \text{Im} \int_{BZ} dk_1 dk_2 n_{\alpha}^k(t) A_i^k(|\phi_{k\alpha}(t)\rangle), \quad (\text{S27})$$

where the weights $n_{\alpha}^k(t)$ are the time dependent population of the α^{th} instantaneous band i.e.,

$$n_{\alpha}^k(t) = \langle \psi_k(t) | c_{k\alpha}^{\dagger}(t) c_{k\alpha}(t) | \psi_k(t) \rangle, \quad (\text{S28})$$

where $c_{k\alpha}(t)$ and $c_{k\alpha}^{\dagger}(t)$ are the annihilation and creation operators respectively, of the eigenmodes of the instantaneous Hamiltonian $H_k(t)$, i.e., $c_{k\alpha}^{\dagger}(t) |0\rangle = |\phi_{k\alpha}(t)\rangle$, where $|0\rangle$ is fermionic vacuum. \tilde{P}_i is the weighted average of the electric polarisation in each band of the time-evolved Hamiltonian $H(t)$; the weights being precisely the time dependent population of each band.

CURRENTS

The definition of the topological classification of out of equilibrium states is directly connected to the evolution of particle currents generated in the time dependent state of the system. For the topological invariant to conform with the adiabatic edge current dynamics, it is essential to take note of the time evolution of the current operator.

As discussed in Refs. [S3, 4], the measured particle current in the out of equilibrium system is dependent on the instantaneous Hamiltonian. This can be easily seen by explicitly computing the expectation of the current operator between two sites when the system is driven out of equilibrium. Referring to the Haldane Hamiltonian and resorting to the Heisenberg picture,

$$\frac{d(a_n^{\dagger} a_m)}{dt} = -i [H(t), a_n^{\dagger} a_m]. \quad (\text{S29})$$

As the dynamics is unitary, the mean rate of change of local population at a site is directly proportional to the average local current at the site. Thus, the expectation,

$$\left\langle \frac{d(a_n^{\dagger} a_m)}{dt} \right\rangle = \sum_n J_{nm}, \quad (\text{S30})$$

where J_{nm} is the average current between the sites i and j . Comparing Eq. (S29) and Eq. (S30), one obtains,

$$J_{nm} = \text{Im} [2H_{nm}(t) \langle a_n^{\dagger} a_m \rangle], \quad (\text{S31})$$

where $H_{nm}(t)$ is the single particle time dependent Hamiltonian,

$$H(t) = \sum_{nm} H(t)_{nm} a_n^{\dagger} a_m, \quad (\text{S32})$$

. To evaluate the edge currents we impose semi-periodic boundary conditions on the 2D lattice. Generically, as defined above, the single particle current can be decomposed as,

$$\langle \vec{J}_{SS} \rangle = \langle \vec{J}_N \rangle + \langle \vec{J}_{NN} \rangle, \quad (\text{S33})$$

where \vec{J}_N and \vec{J}_{NN} are the nearest neighbour and the next nearest neighbour current operators respectively,

$$\begin{aligned} \langle J_{Nn}^x \rangle &= \sum_m t_1 \langle a_n^{\dagger} a_m \rangle - \hbar c \\ \langle J_{NNn}^x \rangle &= \sum_m t_2 \langle a_n^{\dagger} a_m \rangle - \hbar c, \end{aligned} \quad (\text{S34})$$

where $\langle J_{Nn}^x \rangle$ ($\langle J_{NNn}^x \rangle$) is the nearest (next nearest) current at the n^{th} site and the summation indices extends over all nearest (next-nearest) neighbour sites to the n^{th} site. Considering the lattice to be periodically wrapped in the x-direction (see Fig. S2a) while being open in the y-direction, one obtains two arm-chair edges at the ends of the cylinder. We compute the total horizontal current flowing in the periodic x-direction on one of the arm chair edges J_N^x for a $N \times N$ lattice, in the post quench state to re-establish the bulk boundary correspondence which is depicted in Fig. (2) of the main manuscript.

NUMERICAL AND EXPERIMENTAL GENERATION OF THE COUNTER-DIABATIC MASS

The time-dependent generation of the counter-diabatic term in Eq. (12) of the main text can be realised experimentally by a temporal modulation of the nearest neighbour hopping amplitude along a particular direction in the real lattice. In Fig. (2) of the manuscript we explicitly demonstrate this by applying a time dependent modulation to the hopping strength along the direction $\vec{\Delta}_{12}$ while keeping the other two nearest-neighbour and next-nearest neighbour hoppings unaffected,

$$\begin{aligned} t_{\vec{\Delta}_{12}}(t) &= -t_1 - h \times \sin\left(\frac{\pi t}{\tau}\right) \\ t_{\vec{\Delta}_{11}} &= -t_1, \\ t_{\vec{\Delta}_{13}} &= -t_1, \end{aligned} \tag{S35}$$

for the duration of the quench, i.e. $t \in [0, \tau]$ (see Fig. 2 of main manuscript). Such anisotropic modulations can be generated experimentally by applying anisotropic strain on the graphene lattice and then modifying it temporally to open up a controlled gap in the spectrum [S5, 6] which in turn suppresses diabatic excitations while crossing a quantum critical point.

* souvik@iitk.ac.in

- [S1] F. D. M. Haldane, Phys. Rev. Lett. **51**, 605 (1983).
- [S2] S. Coh and D. Vanderbilt, Phys. Rev. Lett. **102**, 107603 (2009).
- [S3] L. D'Alessio and M. Rigol, Nature Communications **6**, 8336 (2015).
- [S4] M. Bukov and A. Polkovnikov, Phys. Rev. A **90**, 043613 (2014).
- [S5] V.M. Pereira, A.H. Castro Neto, Phys. Rev. Lett. **103**, 046801 (2009).
- [S6] M. R. Masir, D. Moldovan, and F. M. Peeters, Solid State Commun. **175-176**, 76 (2013).